

Chapter 4

SIMULATION RESULTS FOR THE IDH

4.1 Introduction

The principle of induction dielectric heating (IDH) has been used in various applications such as brazing, surface hardening, forging, annealing, melting, drying and dehydration for food etc. Each application has different appropriate frequency required. In food application frequency depends on work-pieces geometry and skin depth requirement [13], [60]. A large number of topologies have been developed. Among them, current-fed and voltage-fed inverters are most commonly used [37]. The advantages of current fed inverter are short-circuiting protection capability and superior no-load performance because of its current-limiting DC link characteristic. Voltage-fed or Current-fed inverter for IDH applications have employed many switches such as Thyristors, GTO's, Bipolar power transistor, IGBT's, MCT's, MOSFET's, SIT. Also in recent year, MOSFET are used in induction heating system, which has the advantage of low conduction loss, high speed switching time and very little gate drive power.

When a work-piece is inserted into an induction coil, variation of induction heating load parameters can affect resonant frequency, resulting in reduction of load power. Therefore, it is necessary to track operating frequency in order to obtain high power factor.

This chapter describes the three phase MOSFET based inverter for dehydration of food (lemon) application. The operating frequency has been adjusted by the micro controller to maintain constant leading phase angle when parameters of IDH load are varied. The

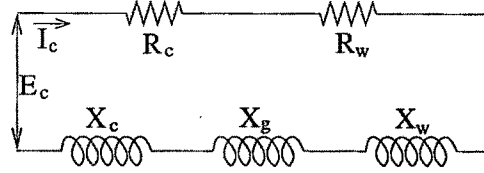


Figure 4.1: The Equivalent Circuit of Induction Coil and Work-piece

output power can be controlled by input setting. The load voltage is controlled to protect the MOSFETs.

4.2 Principle of Induction Dielectric Heating

The IDH method is one of most suitable methods for such heating due to the non-contact between the induction coil and the work-pieces. It is heated by being placed inside the magnetic field, induced in the coil when energized, causes eddy currents in the work-pieces and increases the heating effect. An equivalent circuit of the induction coil and work-piece is shown in Figure 4.1.

$$\text{Work resistance, } R_w = K(\mu_r p A_w) \text{ ohms} \quad (4.1)$$

$$\text{Coil resistance, } R_c = K \left(\frac{k_r \pi d_c \delta_c}{2} \right) \text{ ohms} \quad (4.2)$$

$$\text{Gap reactance, } X_g = K(A_g) \text{ ohms} \quad (4.3)$$

$$\text{Work reactance, } X_w = K(A_r q A_w) \text{ ohms} \quad (4.4)$$

$$\text{Coil reactance, } X_c = K \left(\frac{k_r \pi d_c \delta_c}{2} \right) \text{ ohms} \quad (4.5)$$

$$K = 2\pi f \mu_0 \left[\frac{N_c^2}{l_c} \right] \text{ Ohms per square meter} \quad (4.6)$$

Where

- μ_r = The relative magnetic permeability
 - A_w = The cross section area of work-piece
 - A_g = The area of gap
 - k_r = The coil correction factor that ranging from 1-1.5
 - N_c = The number of turns of induction coil
 - l_c = The length of gap
 - δ_c = The resistivity of copper
 - d_c = The diameters of induction coil
- (p and q are function for a solid cylinder)

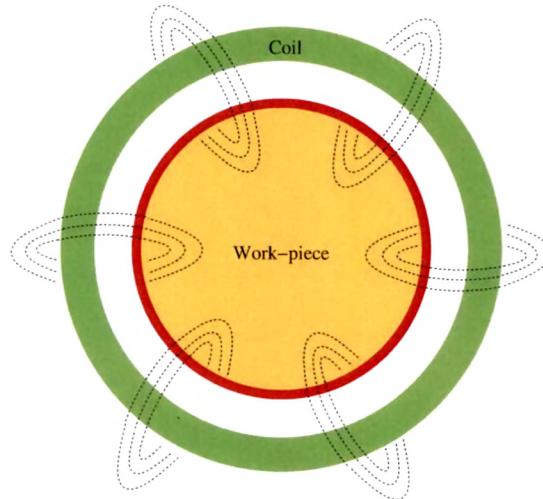


Figure 4.2: Practical Representations of IDH Coil

As shown in Figure 4.1 and from above equations, it can be seen that the parameters of induction heating load (induction coil and work-piece) depend on several variables including the shape of the heating coil, the space between the work-piece and coil, their electrical conductivities and magnetic permeability and the frequency [13], [60].

4.3 System Considerations

This section describes the load impedance characterization of an induction dielectric heating. This impedance model is needed for suitable power supply design. Finally the basic operating limitations of a load, three phase inverter are briefly reviewed [47], [58], [75], [79], [85], [89], [96], [107], [111], [113].

4.3.1 Considerations of coil design

A block diagram of an IDH coil and equivalent circuit modelled are shown in Figure 4.2 and Figure 4.3, respectively. The heating coil is modelled as a transformer with a single turn secondary winding. The equivalent model can be represented in a simplified form by an equivalent induction and resistance. The circuit represented in Figure 4.3 can also be characterized by a dimensionless parameter called the quality factor 'Q' of the coil.

The core rating is generated based on data about the frequency, resistivity, magnetic

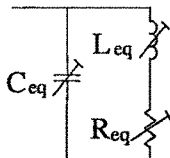


Figure 4.3: Equivalent Electric Circuit Model of IDH Coil

permeability, coil dimensions, coil resistivity and an acceptable lower and upper bound on the number of volts per turn. On the other hand power rating is governed by the heating rate requirement and any additional primary coil losses. The choice for operating frequency is based upon the form in which the solid material enters the pot, the electromagnetic properties of the material and the conducting or non-conducting material. These aforementioned items taken together are often used to identify skin depth of the material. This term corresponds to an effective distance from the surface where induced currents will flow.

Heat will be generated in work-piece and will be partially conducted away to the surrounding medium. The generated and conducted heat can either be used to surface heat the material. The effective parameters for the equivalent resistance and inductance will vary throughout the heating cycle. This comes about as a result of the changes in impedance in the material and also changes in the amount of coil flux coupling the material. The change can also be expressed as a variation in the Q of the coil. Electromagnetic type materials exhibit an increase in Q over the duration of the heating cycle. On the other hand non-magnetic metals exhibit small variations in Q over the duration of the heating cycle. The power supply designers' main objective therefore is to determine the maximum range over which the Q of the coil will vary. The maximum Q at the rated coil voltage is then established as the baseline value for purposes of designing the power supply. Secondly, these base values are then used to specify a transformer turns ratio. The purpose of the transformer is to match as closely as possible the coil voltage to the power supply voltage. Maximum power transfer can be achieved if the reactive component of the load is compensated. This can be done using different circuit topologies incorporating capacitors. Capacitors value can be chosen to compensate for the reactive power assuming a fixed value for the reactive component of the load. Under these conditions the transformer can be matched to the power supply. However exact matching is not the case in practice.

This comes about as a result of a change in the equivalent inductance during a heating cycle. The problem is particularly acute for ferrous metals. Initial coupling between the coil and load is good. However the coupling decreases over a period of time as successive layers of the heated material exceed the Curie point. This gradual process corresponds to a slow decrease in the inductance of the load i.e., (order of minutes). Consequently the power transfer will decrease.

4.3.2 Coil specification

The foregoing discussions can conveniently be summarized in the form of the following coil specifications

1. Coil voltage
2. Power rating
3. Operating frequency
4. Range of Q
5. Range of L_{eq} .

The above design data can in many cases be obtained using simple design rules [60] however, for special cases (for example, partially conducting refractoriness, or coils whose length to width ratio is small) it will be necessary to characterize coil impedance, as a function of frequency, using a finite element software package.

Nevertheless, whichever approach is taken, the requirements are subsequently used for purposes of designing the matching transformer and the power supply.

4.3.3 Power supply requirements

AC to DC rectifier topology (1 or 3 phase) and inverter topology commonly used in IDH is shown in Figure 4.4. It is referred to as either a voltage driven power supply or a current driven power supply. This chapter concerns itself primarily with power supplies that operate on the principle of three phase inverter. The load (comprised of an inductance, capacitances and resistance) should at all times be presenting itself as a leading power factor to the source. Hence the capacitor voltage should lag the driving current source

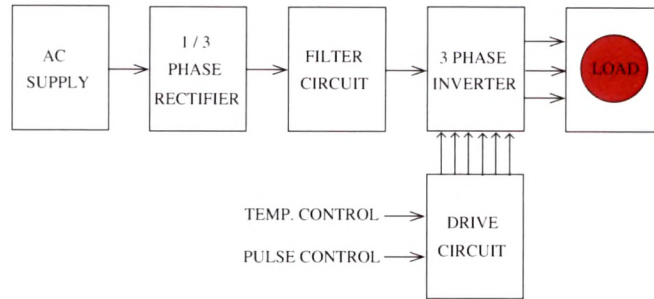


Figure 4.4: Structure of The IDH

inverter. Alternatively the operating frequency should always reside above the resonant frequency of the tuned circuit. Similarly the total current (i_o) for the voltage source driven circuit lead the applied voltage. This is the case if the applied frequency is less than the resonant frequency.

Converters use semiconductor switches such as MOSFET's and IGBT's. The proper operating of the switches requires that a reverse voltage be maintained across the switch, for a minimum interval of time subsequent to the current extinction. This interval is referred to as the turn off time for the device; it is another way of stating a leading power factor load. The power supply control circuit should also guarantee that current and capacitor voltages be maintained within safe operating levels. Finally, the power supply should be able to control and maintain the power applied to the load subject to safe operating conditions. Taken together these operating modes can be summarized as follows.

1. Constant output power operation
2. Capacitor voltage limited operation
3. Load current limited operation
4. Turn off time limited operation
5. Fault operation

4.4 Operation of Proposed Inverter

Figure 4.5 illustrates the power circuit of proposed IDH that employs six switches at primary side of isolating transformer to establish some part of three phase utility voltages on the primary winding. Being the converter supplied by voltage source, the input phases should never be short circuited and owing to presence of inductive loads, the load currents should not be interrupted. With these constrains in 1 phase to 3 phase converter, there are 8 permitted switching combinations, which are shown in Table 4.1

For each combination, the input and output line voltages can be expressed in term of space vectors as

$$v_i = \frac{2}{3} (v_{ab} + v_{bc}e^{j2\pi/3} + v_{ca}e^{j4\pi/3}) = V_i e^{j\alpha_i} \quad (4.7)$$

$$v_o = \frac{2}{3} (v_{AB} + v_{BC}e^{j2\pi/3} + v_{CA}e^{j4\pi/3}) = V_o e^{j\alpha_o} \quad (4.8)$$

In the same way, the input and output line currents can be expressed as given below.

$$i_i = \frac{2}{3} (i_a + i_b e^{j2\pi/3} + i_c e^{j4\pi/3}) = I_i e^{j\beta_i} \quad (4.9)$$

$$i_o = \frac{2}{3} (i_A + i_B e^{j2\pi/3} + i_C e^{j4\pi/3}) = I_o e^{j\beta_o} \quad (4.10)$$

It may be noted from above equations that the resulting output voltage has been expressed as a function of the input voltages and the resulting input current of primary side has been represented as function of the output currents of secondary side.

As shown in Table 4.1, for the 6 combinations of group I, each output phase is connected to a different input phase. In the 2 combinations of group II, all the output phase is short-circuited.

Each combination of group I determines an output voltage vector having a phase angle α_o which is dependent on the phase angle α_i of the corresponding input voltage vector. In the same way, the input current vector has phase angle β_i which is related to the phase angle β_o of the output vector. Hence, in order to apply the SVM technique, these combinations cannot be usefully employed.

Finally, the 2 configurations of group II determine zero output voltage and zero input current vectors.

Duration of non zero intervals, T_{ON} , are given by equation 4.11:

$$t_{ON} = D(kT_s) \frac{T_s}{2} \quad (4.11)$$

Table 4.1: Switching Vectors, Phase Voltages and Output Line to Line Voltage

Voltage Vectors	Switching Vector			Line to Neutral Voltage			Line to line voltage		
	a	b	c	V_{ab}	V_{bc}	V_{ca}	V_{ab}	V_{bc}	V_{ca}
Group I									
V_1	1	0	0	2/3	-1/3	-1/3	1	0	-1
V_2	1	1	0	1/3	1/3	-2/3	0	1	-1
V_3	0	1	0	-1/3	2/3	-1/3	-1	1	0
V_4	0	1	1	-2/3	1/3	1/3	-1	0	1
V_5	0	0	1	-1/3	-1/3	2/3	0	-1	1
V_6	1	0	1	1/3	-2/3	1/3	1	-1	0
Group II									
V_0	0	0	0	0	0	0	0	0	0
V_7	1	1	1	0	0	0	0	0	0

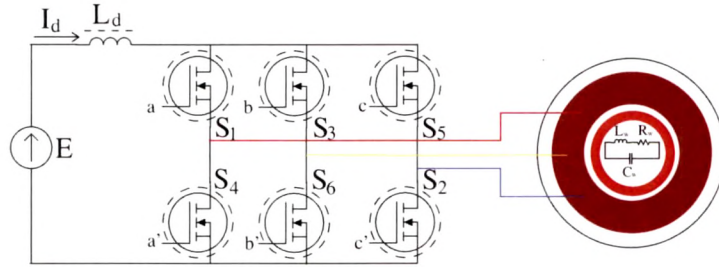


Figure 4.5: Three Phase Inverter for IDH

$$D(kT_s) = \frac{V_{ref}}{v_{\max}(kT_s)} \quad (4.12)$$

Where

T_s = Switching period

D = Duty cycle

V_{ref} = Reference adjusting voltage

Secondary side of isolation transformer is coupled to parallel resonance tank circuit through matching (or filter) coil L_C .

4.5 Analysis of Three Phase Inverter

The three phase inverter is shown in Figure 4.5. Its analysis is based on the following assumptions:

1. The quality factor of three phase inverter load $Q = \omega L_w / R_w$ is larger than 2.5 (high Q load).
2. The inverter circuit inductance ratio factor $(L_d / L_w) > 10$.
3. The three phase inverter switches are ideal.
4. The internal resistance of the three phase inverter DC source is negligible.

The transient behaviour of the IDH circuit represented by the following Laplace transformer equations:

$$\begin{aligned}
 sL_d I_d(s) + (-1)^{n-1} U_c(s) &= \frac{E}{s} + L_d i(0) \\
 -U_c(s) + (R_w + sL_w) I(s) &= L i(0) \\
 -(-1)^{n-1} I_d(s) + C_w s U_c(s) + I(s) &= C_w u_c(0)
 \end{aligned} \tag{4.13}$$

Where

$$\begin{aligned}
 I_d(s) &= \text{The Laplace transforms of the three phase inverter input current } i_d(t) \\
 I(s) &= \text{Load current } i(t) \\
 U_c(s) &= \text{Voltage } u_c(t)
 \end{aligned}$$

With their initial values $i_d(0)$, $i(0)$, $u_c(0)$ and $(-1)^{n-1}$ is a sign changing factor, reflecting to the three phase inverter switching, where n is a number of half periods counting from inverter starting instant ($n_{st} = 1$)

The solution of the IDH system equation 4.13 is

$$I_d(s) = \frac{1}{sL_d L_w C_w M(s)} [(C_w L_w s^2 + C_w R_w s + 1)E + A_{I_d}] \tag{4.14}$$

$$U_c(s) = \frac{(-1)^{n-1} (R_w + L_w s)}{sL_d L_w C_w M(s)} (E - A_{u_c}) \tag{4.15}$$

$$I(s) = \frac{(-1)^{n-1}}{sL_d L_w C_w M(s)} (E + A_I) \tag{4.16}$$

Where

$$M(s) = s^3 + \frac{R_w}{L_w} s^2 + \frac{L_d + L_w}{L_d L_w C_w} s + \frac{R_w}{L_d L_w C_w} \tag{4.17}$$

and A_{I_d} , A_I and A_{U_c} are the corresponding initial condition polynomials:

$$A_{I_d} = (L_d L_w C_w s^3 + L_d R_w C_w s^2 + L_d s) i_d(0) - (-1)^{n-1} (L_w C_w s^2 + R_w C_w s) u_c(0) + (-1)^{n-1} s L_w i(0) \quad (4.18)$$

$$A_I = L_d s i_d(0) + (-1)^{n-1} L_d C_w s^2 u_c(0) + (-1)^{n-1} (L_d L_w C_w s^3 + L_w s) i(0) \quad (4.19)$$

$$A_{U_c} = -L_d s i_d(0) - (-1)^{n-1} L_d C_w s^2 u_c(0) + (-1)^{n-1} \frac{L_d L_w s^2}{L_w s + R_w} i(0) \quad (4.20)$$

For the first half period

$$A_{I_d} = A_I = A_{U_c} = 0$$

To obtain the values of $I_d(s)$, $U_c(s)$ and $I(s)$ it is essential to obtain the roots of equation 4.17. It is preferable to normalize parameters.

The inductance ratio factor is defined as:

$$K = \frac{L_d}{L_w} \quad (4.21)$$

a load quality factor and a resonant frequency

$$Q = \frac{\omega_0 L_w}{R_w} \quad (4.22)$$

$$(4.23)$$

Where

$$\omega_0 = \frac{1}{\sqrt{L_w C_w}} \quad (4.24)$$

and a normalized frequency

$$\eta_f = \frac{\omega}{\omega_n} \quad (4.25)$$

Where

ω_n = The natural angular frequency

Power consumption of 10 – 1000kW with frequency range of 0.5 to 10MHz the range of Q , K and η_f has been provided by equation 4.26.

$$2.5 < Q < 20$$

$$10 < K < 200 \quad (4.26)$$

$$1.01 < \eta_f < 1.1$$

Therefore, the approximate analytical expressions for three phase inverter currents and voltage $i_d(t)$, $i(t)$ and $u_c(t)$ are obtained for these ranges of parameters.

The characteristic equation as described in equation 4.17 having order more than two needs iterative method is non-linear algebraic equation. According to this method, the third-order equation of the form

$$s^3 + k_1s^2 + k_2s + k_3 = 0 \quad (4.27)$$

after separating the real root $s_1 = -a$ may be written as

$$(s + a)[s^2 + (k_1 - a)s + (k_2 - b)] = 0 \quad (4.28)$$

Performing all the operations in equation 4.28 and comparing the coefficients of equal powers of s in equation 4.27 and equation 4.28,

$$b = (k_1 - a)a \quad (4.29)$$

$$a = \frac{k_3}{k_2 - b} \quad (4.30)$$

Thus, from equation 4.29 and equation 4.30 unknowns are a and b . To find them, the iteration method is used. Start with a zero iteration value: $a_0 = 0$, which gives in accordance with equation 4.29 $b_0 = 0$ and then, in accordance with equation 4.30, the first iteration value of a is $a_1 = k_3/k_2$. The next iteration value of b , i.e., b_1 is substituting value into equation 4.29. Hence, the following recurrent formula for the real root a_{j+1} can be employed:

$$a_{j+1} = \frac{k_3}{k_2 - b_j} \quad (4.31)$$

Where

$$b_j = (k_1 - a_j)a_j \quad (4.32)$$

and $j = 0, 1, 2, \dots$ is the number of iterations. This iteration process is repeated up to the required accuracy.

Substituting, equation 4.21, equation 4.22 into equation 4.17 yields

$$M(s) = s^3 + \frac{\omega_0}{Q}s^2 + \frac{\omega_0^2(K+1)}{K}s + \frac{\omega_0^3}{KQ} = 0 \quad (4.33)$$

Thus, the coefficients of equation 4.27 are

$$k_1 = \frac{\omega_0}{Q} \quad (4.34)$$

$$k_2 = \frac{\omega_0^2(K+1)}{K} \quad (4.35)$$

$$k_3 = \frac{\omega_0^3}{KQ} \quad (4.36)$$

Starting with $a_0 = 0$ and $b_0 = 0$, in accordance with equation 4.31

$$a_1 = \frac{k_3}{k_2} = \frac{\omega_0}{Q(K+1)} \quad (4.37)$$

and with equation 4.32

$$b_1 = (k_1 - a_1)a_1 = \frac{\omega_0^2 K}{Q^2(K+1)^2} \quad (4.38)$$

The accuracy of root iteration may be estimated by applying a conversion rate factor $d_i = a_j/a_{j+1}$. At the first iteration:

$$d_1 = \frac{a_1}{a_2} = 1 - \frac{b_1}{k_2} = 1 - \frac{K^2}{Q^2(K+1)^3} \quad (4.39)$$

The limit accuracy is $d_\infty = 1$, which means that the root value was calculated exactly. As can be seen from equation 4.39 d_1 approaches one as Q and K become larger. Substituting into equation 4.39 the lowest values of Q and K equation 4.26.

$$d_1 \simeq 1 - \frac{1}{Q^2 K} = 1 - 0.61 * 10^{-1} = 0.984$$

Thus, even under adverse conditions, i.e., by using the lowest Q and K , the accuracy of the first iteration is sufficient. Therefore

$$s_1 = -a_1 \simeq -\frac{\omega_0}{Q(K+1)} \quad (4.40)$$

Substituting now equation 4.37 and equation 4.38 into the second factor of equation 4.28 yields the following quadrant equation:

$$s^2 + \frac{\omega_0 K}{Q(K+1)} s + \frac{\omega_0^2(K+1)}{K} = 0 \quad (4.41)$$

Which gives the next two roots:

$$s_{2,3} = \gamma \pm j\omega_n = \frac{\omega_0 K}{2Q(K+1)} \pm j\omega_0 \sqrt{\frac{K+1}{K}} \quad (4.42)$$

Where

$$\omega_n = \omega_0 \sqrt{\frac{K+1}{K}} = \text{The natural angular frequency}$$

With roots equation 4.41, equation 4.42 the solution of equation 4.14, equation 4.15 and equation 4.16 is

$$\begin{aligned} i_d(t) &= \frac{E}{R} [1 + A_1 e^{-\frac{\omega_0 t}{Q(K+1)}} + A_2 e^{-\frac{\omega_0 K t}{2Q(K+1)}} \cos(\omega_n t + \alpha_1)] \\ u_c(t) &= E [1 + B_1 e^{-\frac{\omega_0 t}{Q(K+1)}} + B_2 e^{-\frac{\omega_0 K t}{2Q(K+1)}} \cos(\omega_n t + \alpha_2)] \\ i(t) &= \frac{E}{R} [1 + C_1 e^{-\frac{\omega_0 t}{Q(K+1)}} + C_2 e^{-\frac{\omega_0 K t}{2Q(K+1)}} \cos(\omega_n t + \alpha_3)] \end{aligned} \quad (4.43)$$

Where $A_1, A_2, \alpha_1, B_1, B_2, \alpha_2, \dots$ are constants of integration or residues, which are dependent on the initial conditions and may be found with the partial-fraction expression techniques. In the first half period the initial conditions equation 4.18, equation 4.19 and equation 4.20 are zero. Taking the residues of the both the real and complex poles and after simplifying due to the conditions imposed by equation 4.21 to equation 4.26, we obtain the values of the first half period:

$$i_d(T/2) = \frac{E}{R} \left(1 - e^{-\frac{\pi}{(K+1)Q\eta_f}} \right) \quad (4.44)$$

$$u_c(T/2) = E \left(1 - \frac{K}{K+1} e^{-\frac{\pi}{(K+1)Q\eta_f}} + \frac{\sqrt{\frac{Q^2}{Q^2+1}}}{K} e^{-\frac{\pi K \sqrt{\frac{K}{K+1}}}{2Q(K+1)\eta_f}} \cos\left(\frac{\pi}{\eta_f} + \phi_1 + \phi_2\right) \right) \quad (4.45)$$

$$i(T/2) = \frac{E}{R} \left(1 - e^{-\frac{\pi}{(K+1)Q\eta_f}} + \frac{1}{K\sqrt{3.06 + Q^2}} e^{-\frac{\pi K \sqrt{\frac{K}{K+1}}}{2Q(K+1)\eta_f}} \cos\left(\frac{\pi}{\eta_f} + \phi_2\right) \right) \quad (4.46)$$

Where

$$\begin{aligned} \phi_1 &= \arctan(2Q) \\ \phi_2 &= \arctan(2Q/3.5) \\ \eta_f &= \omega/\omega_n \end{aligned}$$

It is the normalized frequency or operating frequency factor and ω is the inverter operating angular frequency.

According to equation 4.45 the first commutation reverse voltage may be estimated. Expressions equation 4.44, equation 4.45 and equation 4.46 allow us to calculate the initial conditions for the second half period of the three phase inverter start up.

To check the accuracy of the above approximate formulas computer aided simulation of the transient behaviour of the inverter in its starting process was performed. The differential equation 4.13 has been solved by the Runge Kutta method and the results

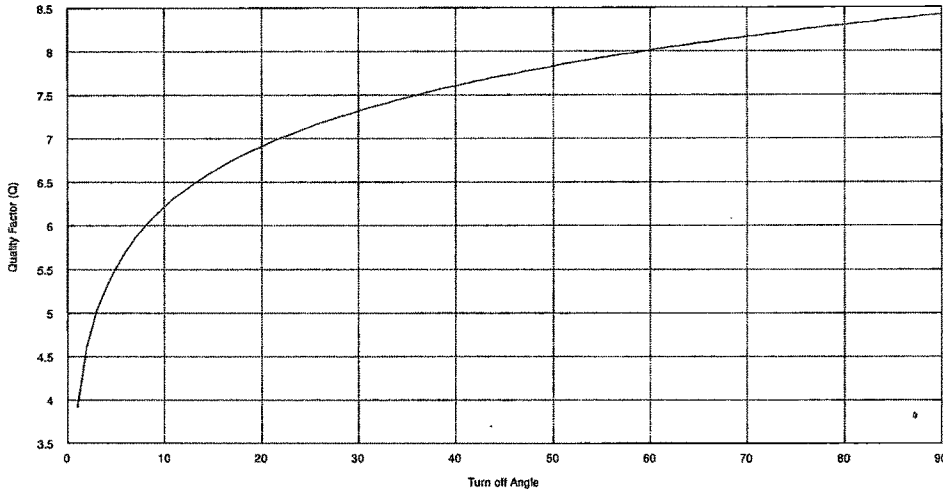


Figure 4.6: The Region of the Three Phase Inverter Parameters Q and β_s Determine the Starting Process

obtained by this computation were compared with the results obtained by approximate formulas equation 4.44, equation 4.45 and equation 4.46. The difference in the results at the end of the first half period is less than 5%. When $Q = 10$, $K = 100$, error is less than 1%. It is evident that this accuracy is high enough for the practical inverter analysis.

The turn off (dead time) angle β_d is of most importance for the reliable start-up process. This angle represents the time ($t_{off} = \beta_d/\omega$) that is available for the reliable switching of the inverter MOSFET's.

The computer-aided turn-off angle β_d shows that its varying may be monotonous or oscillating, depending on the circuit parameters and operating frequency factor. By the monotonous change the turn-off angle β_{dmin} takes place at the second commutation cycle. However, by the oscillating change it takes place at the following half-periods. Figure 4.6 shows two regions of the inverter parameters, i.e., Q and steady state turn off angle β_s which determine the kind of angle β_d changing. The steady state turn off angle β_s is related to the factor η_f [16] as

$$\tan\beta_s = \left(\eta_f - \frac{1}{\eta_f}\right) Q \quad (4.47)$$

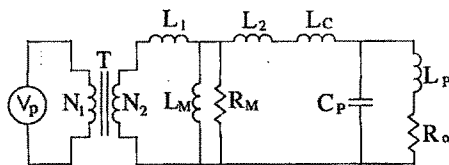


Figure 4.7: Circuit of Proposed IDH Equivalent

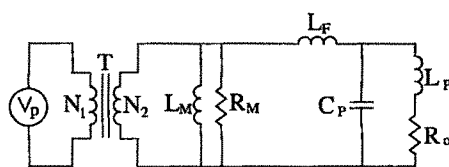


Figure 4.8: Simplified Circuit

Thus, for the known β_s , the frequency factor η_f may be determined with equation 4.22 and taking into account that $\eta_f = \omega/\omega_n$ and $\omega_n = \omega_0\sqrt{(K+1)/K}$, as

$$\eta_f = \left(1 - \frac{\sqrt{\frac{K+1}{k}} R \tan \beta_s}{2\pi f L_w}\right)^{-\frac{1}{2}} \quad (4.48)$$

When η_f changes from 1.01 to 1.1 [see (equation 4.26)], β_s changes from 5° to 75° in equation 4.47.

4.6 Calculation of Switching Frequency

Circuit of proposed 3 phase IDH equivalent to switching transformer (ST) is shown in Figure 4.7. R_M indicates core losses. L_M , L_{l1} and L_{l2} are mutual and leakage inductances of isolation transformer. Figure 4.8 shows the simplified circuit where L_F is obtained as follows:

$$L_F = L_C + L_{l1} + L_{l2} \quad (4.49)$$

Secondary side of isolation transformer provides a rectangular voltage V_S . An LC circuit feeds an inductive load with typical power factor less than 0.1 [94]. Parallel resonance

tank equivalent impedance matching coil is given by

$$Z_T(j\omega) = j\omega L_F + \frac{1}{j\omega C_P + \frac{1}{j\omega L_P + R_o}} \quad (4.50)$$

To obtain proper switching angular frequency, ω_0 , imaginary part of equation 4.50 should be taken equal to zero. Due to low power factor of the induction coil, it is possible to assume $R_o^2 \ll (\omega_0 L_P)^2$, therefore equation 4.50 can be simplified as equation 4.51:

$$Z_T(j\omega) \approx j\omega L_F + \frac{\frac{R_o}{\omega_0^2 L_P^2} - j\omega_0 \left[C_P - \frac{1}{\omega_0^2 L_P} \right]}{\omega_0^2 \left[C_P - \frac{1}{\omega_0^2 L_P} \right]^2} \quad (4.51)$$

Imaginary part of equation 4.51, taken equal with zero, is solved to obtain f_0 by the following equation:

$$\omega_0 = \sqrt{\frac{L_P + L_F}{C_P L_P L_F}}; \omega_0 = 2\pi f_0 \quad (4.52)$$

Equation 4.52 shows the proper switching frequency, f_0 , to transfer maximum power to the load. The value of impedance Z_T at frequency f_0 is obtained as equation 4.53:

$$Z_T(j\omega) \approx R_o \left(\frac{L_F}{L_P} \right)^2 \quad (4.53)$$

Maximum transferred power to R_o at switching frequency f_0 , is achieved by equation 4.51. V_{S1} and N_2/N_1 are effective main components of secondary voltage and winding ratio of transformer, respectively.

$$P_O = \frac{V_S^2}{Z_T(j\omega_0)} \approx \frac{V_{S,1}^2}{R_o \left(\frac{L_F}{L_P} \right)^2} \quad (4.54)$$

$$P_O \approx \left(\frac{2\sqrt{2}}{\pi} \cdot \frac{N_2}{N_1} \cdot \frac{L_P}{L_F} \right)^2 \cdot \frac{V_{ref}^2}{R_o}$$

It is clear from equation 4.54 that output can also be determined by winding ratio of high frequency transformer. Also the type of isolation transformer must be selected according to operation frequency.

4.7 Calculation of Matching Coil Value

There are several methods to determine matching coil value. To obtain a good filtering performance of output stage and almost sinusoidal waveform on the induction coil,

Table 4.2: Circuit Parameters

Parameter	Value	Parameter	Value
Utility	380V/50Hz	N_1/N_2	1
V_{ref}	300V	L_F	200 μ H
L_P	10 μ H	C_P	26.96 μ F
R_o	50m Ω	L_M	20mH

following relationship may be assumed.

$$L_F \gg L_P \quad (4.55)$$

Also, start-up current must be limited by L_F . The maximum possible start-up primary current variation, neglecting transformer inrush current, can be approximated by equation 4.56:

$$\max \Delta I_{primary\ startup} \approx \frac{1}{L_F} \left(\frac{N_2}{N_1} \right)^2 \frac{T_s}{2} \sqrt{2} V_m \quad (4.56)$$

V_m is the peak voltage of the utility. Maximum allowable switching devices current found from the specifications supplied by manufacturer must be greater than maximum primary start-up current. Thus L_F can be determined by considering equation 4.55 and equation 4.56.

4.8 Simulation Results

Sample circuit parameters are given by Table 4.2. The switching frequency calculated from equation 4.52 is 9931.80Hz. Consequently, from equation 4.50 we have $Z_T(j\omega_o) = 1.969 \angle -10^\circ$, which gives a power factor close to 1 (0.9999) as shown in Figure 4.9. Figure 4.10, Figure 4.11, Figure 4.12 and Figure 4.13, Figure 4.14, Figure 4.15 show waveforms of supply voltage and primary side output voltage, respectively. Secondary side of isolation transformer, load voltage and induction coil current are shown in Figure 4.16, Figure 4.17, Figure 4.18 and Figure 4.19, Figure 4.20, Figure 4.21 respectively. Simulation summaries are given in Table 4.3. Figure 4.22, Figure 4.23, Figure 4.24 show FFT of output voltages.

Table 4.3: Simulation Summaries

Parameter	Value	Parameter	Value
V_{ab}	84.874V	I1	92.275A
V_{bc}	84.882V	I2	92.274A
V_{ca}	84.883V	I3	92.265A
PF	0.9999	THD(V_o)	0.7%
F_s	9956Hz	Pout	7831.61W

Table 4.4: Simulation Results

Frequency in Hz	Output Voltage in volt
0.5k	732.00
1.0k	416.24
1.5k	324.20
2.0k	159.41
5.0k	90.50
10.0k	84.874

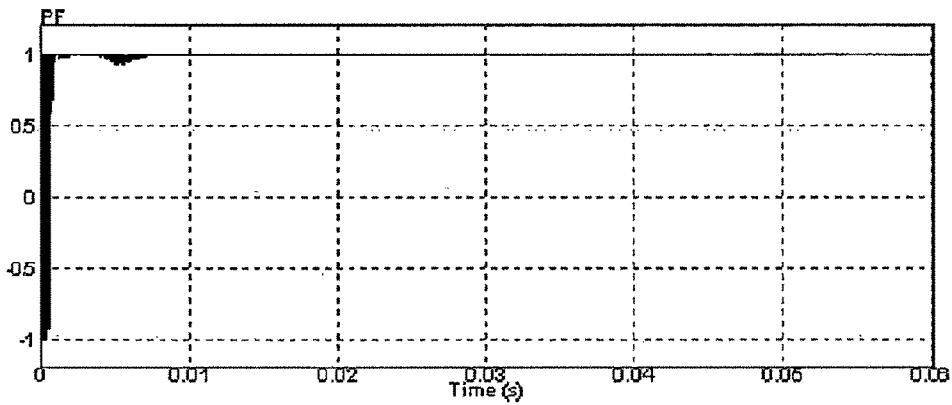


Figure 4.9: Power Factor

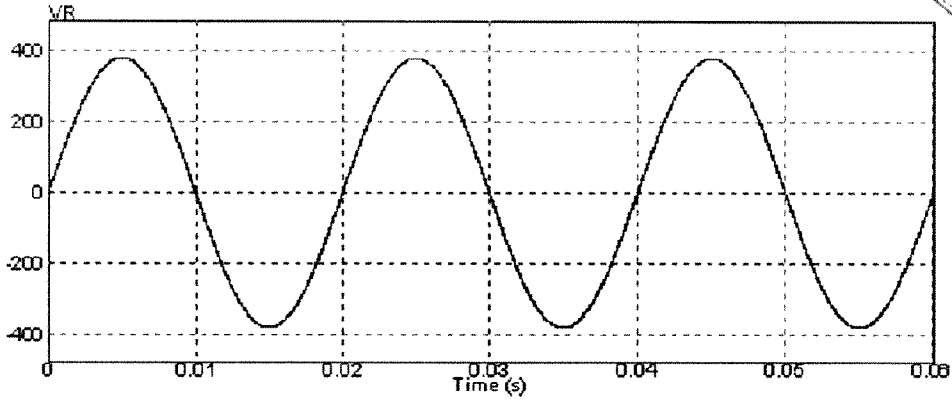


Figure 4.10: R Phase Supply Voltage Waveform

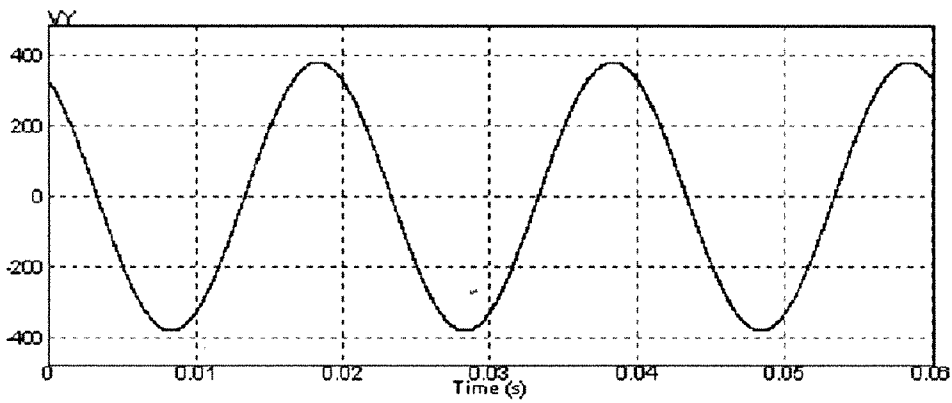


Figure 4.11: Y Phase Supply Voltage Waveform

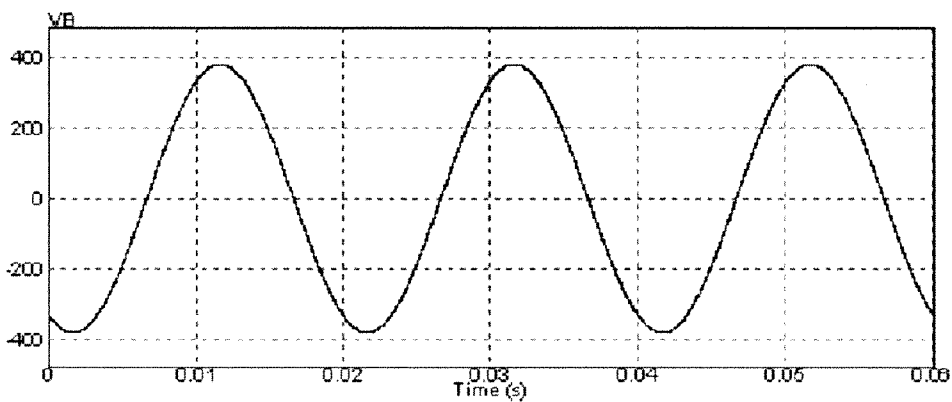


Figure 4.12: B Phase Supply Voltage Waveform

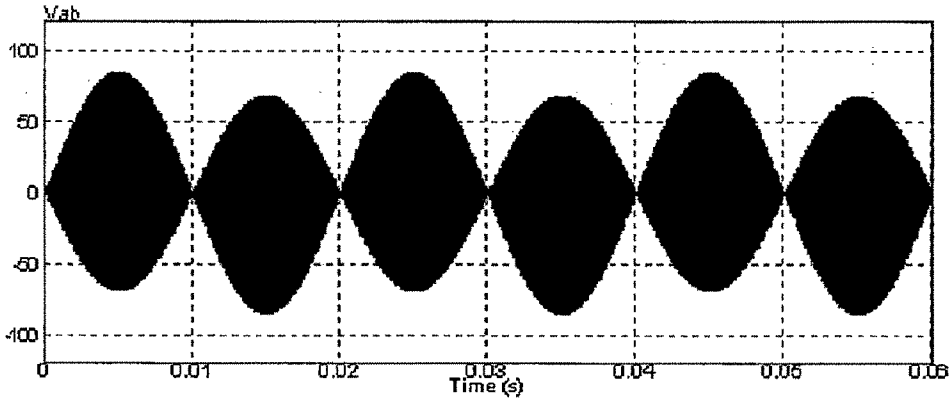


Figure 4.13: Waveform of Primary Output Voltage for V_{ab}

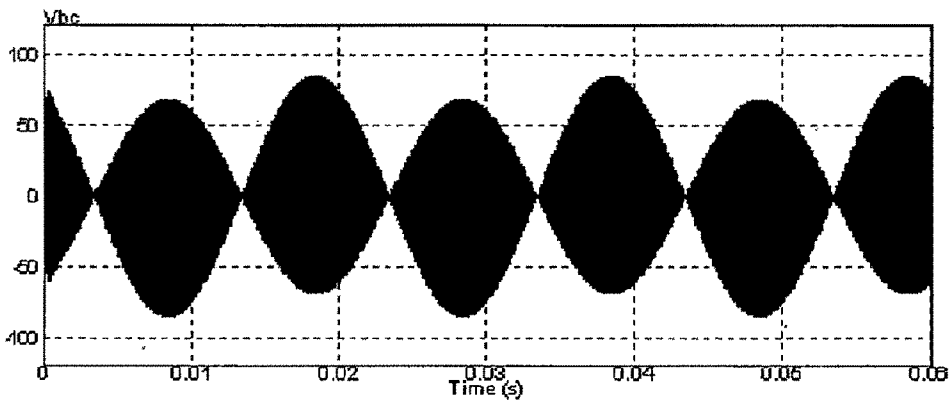


Figure 4.14: Waveform of Primary Output Voltage for V_{bc}

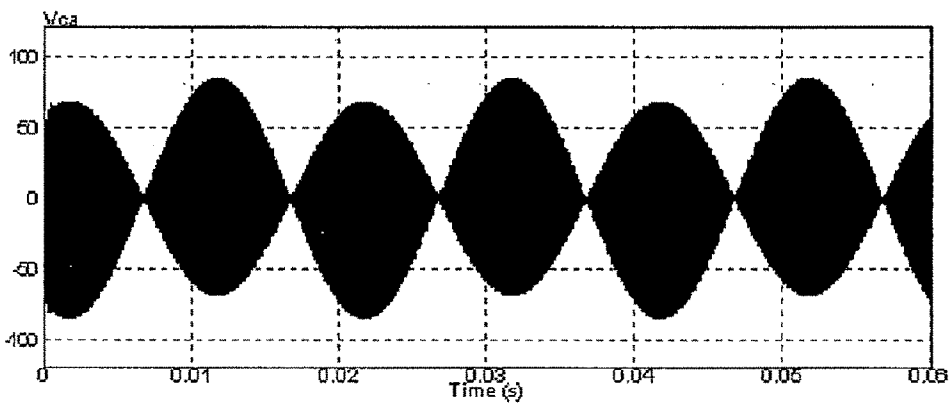


Figure 4.15: Waveform of Primary Output Voltage for V_{ca}

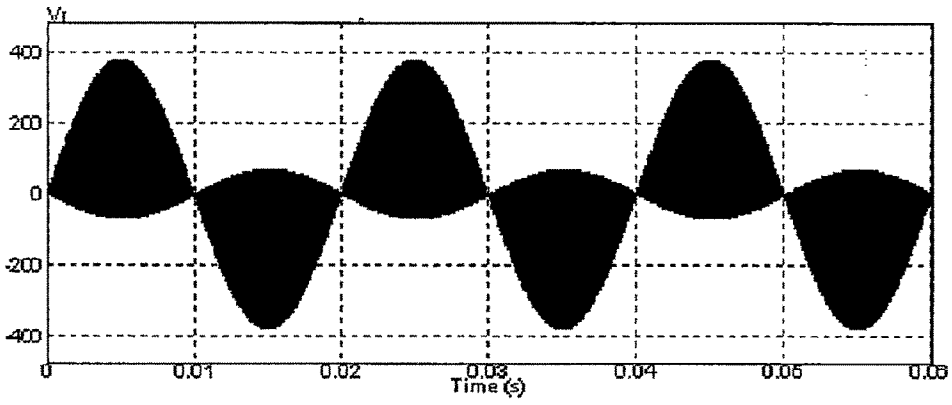


Figure 4.16: Secondary Side Output Voltage V_r

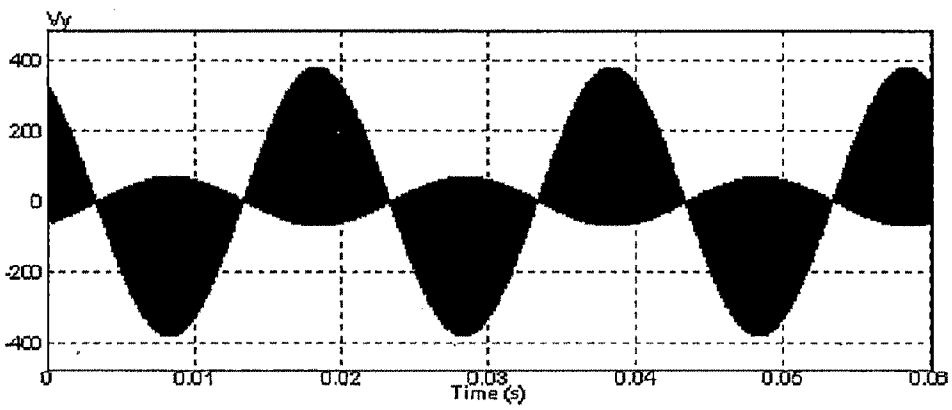


Figure 4.17: Secondary Side Output Voltage V_y

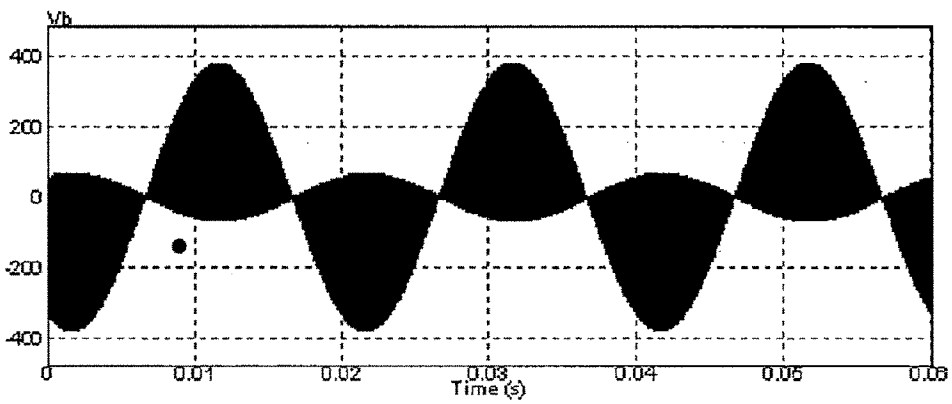


Figure 4.18: Secondary Side Output Voltage V_b

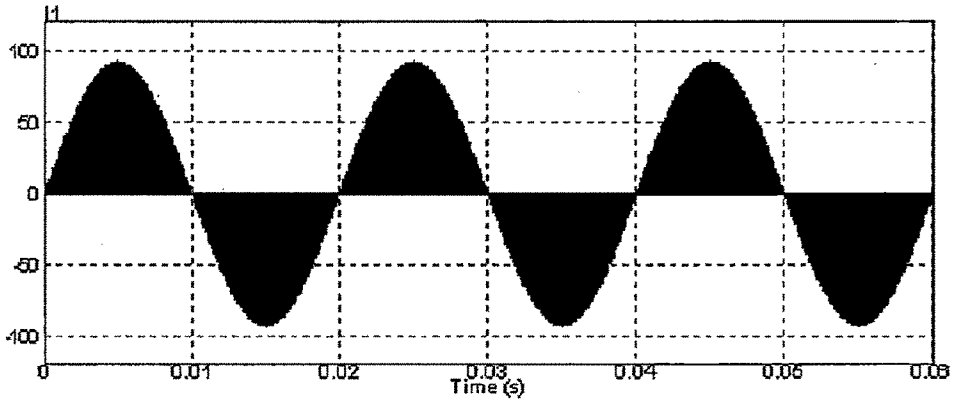


Figure 4.19: Induction Coil Current I_1

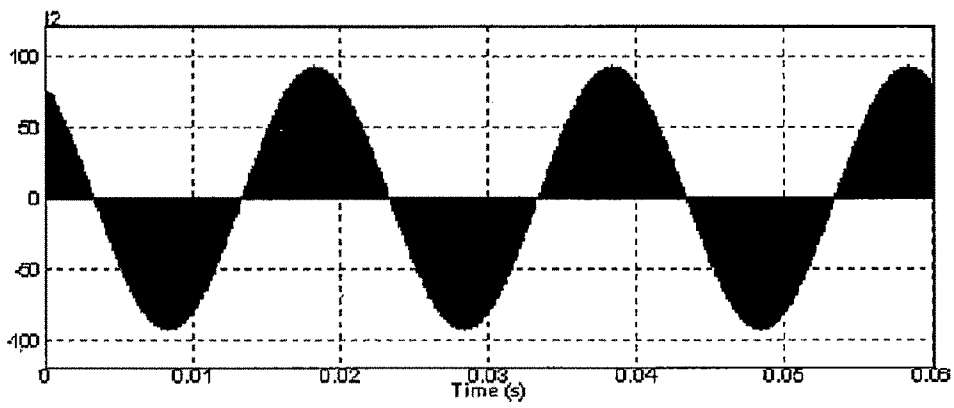


Figure 4.20: Induction Coil Current I_2

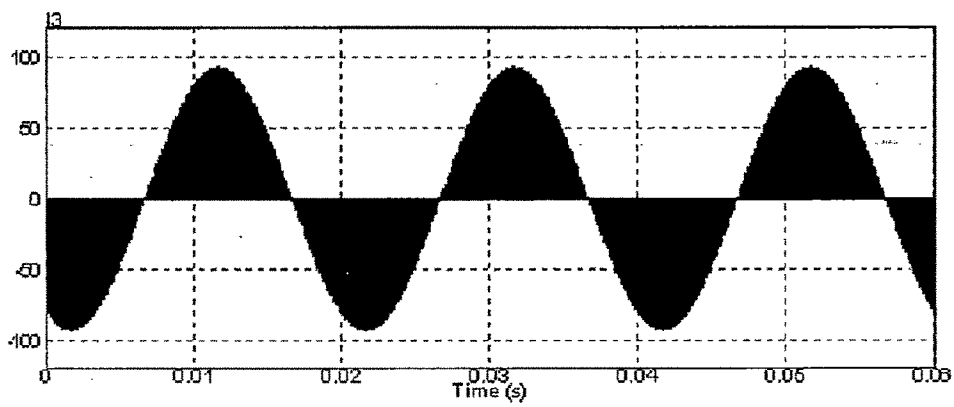


Figure 4.21: Induction Coil Current I_3

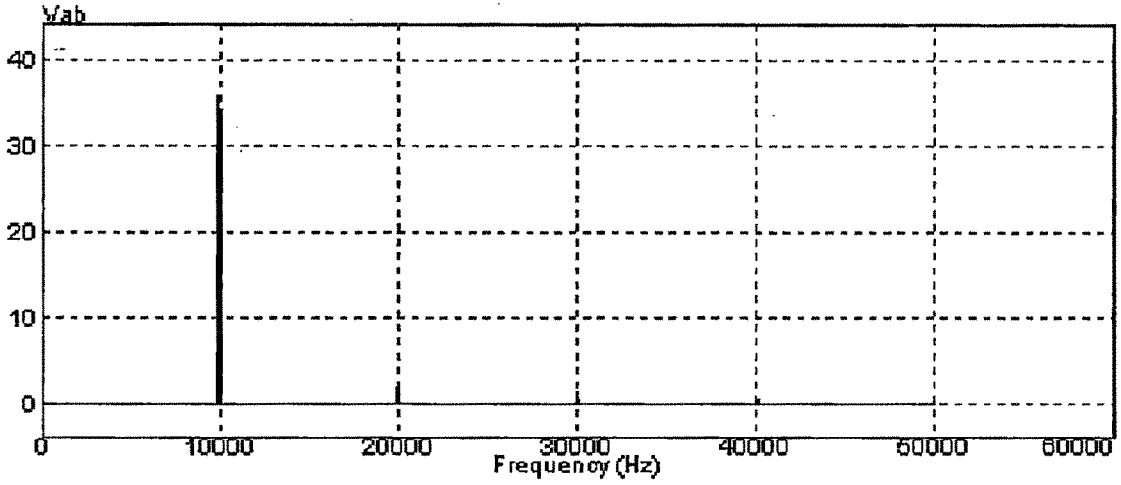


Figure 4.22: FFT of Output Voltage for V_{ab}

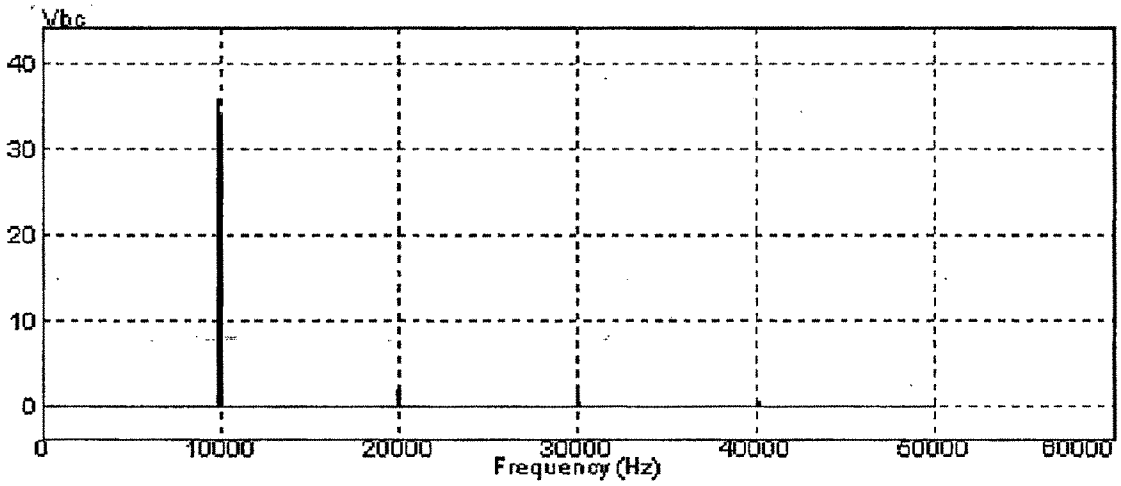


Figure 4.23: FFT of Output Voltage for V_{bc}

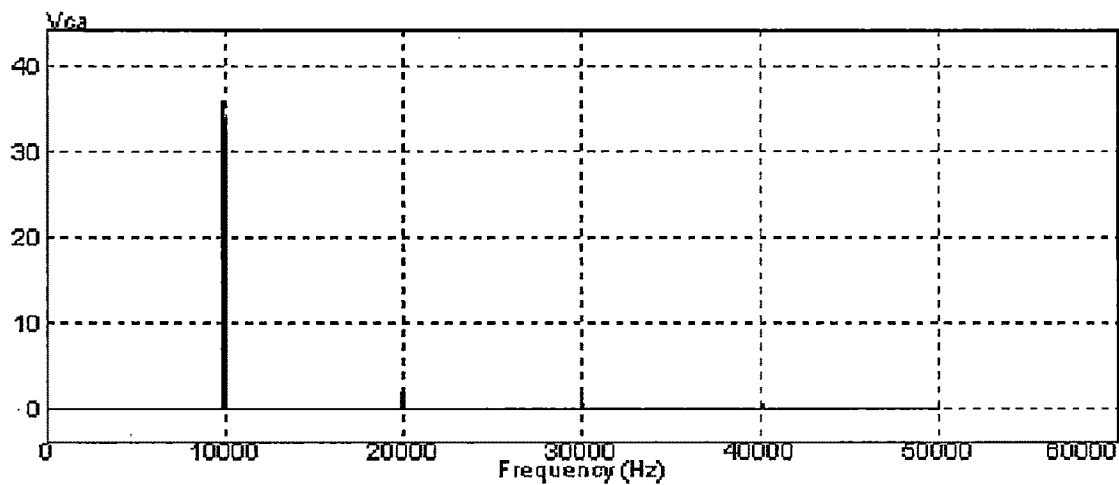


Figure 4.24: FFT of Output Voltage for V_{ca}

4.9 Conclusions

In this chapter an induction dielectric heating device with high frequency transformer structure has been described. Comparison of proposed circuit has been carried out both by mathematical analysis and by simulation. The result shows that value of power factor obtained is unity. Flexibility aspects of switching transformer leads to several advantages such as unity power factor without using any reactive element, symmetric loading from utility point of view, isolation of working coil, compact dimensions and almost uniform sinusoidal output.

Additionally, this topology can provide any voltage level conversion ability, which leads to desired power even at low input voltage levels. Furthermore, proposed topology provides maximum output power and reduced THD utilization. This requires comparatively smaller size of matching filter coil which work suitably with auto tuning switching frequency controller.